Attenuation of ER stress prevents post-infarction-induced cardiac rupture and remodeling by modulating both cardiac apoptosis and fibrosis

Tao Luo[a,e,*], **Jin Kyung Kim**[a], **Baihe Chen**[b], **Ahmed Abdel-Latif**[c], **Masafumi Kitakaze**[d], and **Liang Yan**[e]

[a]Division of Cardiology, Department of Medicine, University of California Irvine Medical Center, Orange, CA 92868, USA

[b]Department of Cardiology, Nanfang Hospital, Southern Medical University, Guangzhou 510515, China

[c]Saha Cardiovascular Research Center, University of Kentucky, Lexington 40536-0509, USA

[d]Department of Clinical Research and Development, National Cerebral and Cardiovascular Center, 5-7-1 Fujishirodai, Suita 5675-8565, Japan

[e]Department of Pathophysiology, Key Laboratory of State Administration of Traditional Chinese Medicine of the People's Republic of China, School of Medicine, Jinan University, Guangzhou 510632, China

Abstract

Endoplasmic reticulum (ER) stress is implicated in the pathophysiology of various cardiovascular diseases, but the role of ER stress in cardiac rupture and/or remodeling after myocardial infarction (MI) is still unclear. Here we investigated whether ER stress plays a major role for these processes in mice. We ligated the left coronary artery (LCA) without reperfusion in mice and administered either NaCl or 4-phenylbutyric acid (4-PBA, 20 mg/kg/d) intraperitoneally for 4 weeks. Cardiac rupture rates during the first week of MI were 37.5% and 18.2% in the control and 4-PBA groups, respectively. The extent of ventricular aneurysm and fibrosis was less, and the cardiac function better, in the 4-PBA group compared with the control group. The protein levels of ER stress markers in the heart tissues of the control group remained elevated during the entire 4-week period after MI, while pro-apoptotic proteins mainly increased in the early phase, and the pro-fibrotic proteins markedly increased in the late phase post MI; 4-PBA decreased all of these protein levels. In the primary cultured neonatal rat cardiomyocytes or fibroblasts, hypoxia (3% O_2) increased the number of apoptotic cardiomyocytes and promoted the proliferation and migration of fibroblasts, all of which were attenuated by 4-PBA (0.5 mM). These findings indicate that MI induces ER stress and provokes cardiac apoptosis and fibrosis, culminating in cardiac rupture and remodeling,

*Corresponding author at: Division of Cardiology, Department of Medicine, University of California Irvine Medical Center, Orange, CA 92868, USA. Tel.: +1 949 824 1495; fax: +1 949 824 1316. luot5@uci.edu (T. Luo).

Conflict of Interest

The authors declare that there are no conflicts of interest.

Transparency Document

The Transparency document associated with this article can be found in the online version.

and that the attenuation of ER stress could be an effective therapeutic target to prevent post-MI complications.

1. Introduction

In patients who suffer acute myocardial infarction (AMI), fatal cardiac rupture can occur within days post infarct, and accounts for 10–20% of all in-hospital cardiac deaths [1–3]. AMI causes the loss of cardiomyocytes followed by proliferation of non-cardiomyocytes and inflammation, leading to cardiac rupture and/or negative remodeling [4]. In animal models, cardiac rupture is observed to occur as high as 24% and 60–75% in C57BL/6 and 129sv mice within the first week of AMI, respectively [5]. While rupture of the ventricle is one of the most fatal acute sequelae of MI, a more insidious, chronic outcome for those surviving the incident MI is negative cardiac remodeling. The excessive remodeling that occurs after loss of cardiomyocytes involves fibrosis and scarring, and eventually impairs systolic and diastolic functions [6,7]. Though it is imperative to prevent these adverse outcomes, the mechanisms for infarct-induced cardiac rupture and remodeling are complicated and far from clear. One of the implicated mechanisms is stress response mediated by the endoplasmic reticulum (ER), a cellular organelle responsible for protein folding, calcium homeostasis, and lipid biosynthesis. Stimuli such as oxidative stress [8,9], ischemic insult [10], disturbances in calcium homeostasis [11] and altered expression of normal and/or folding-defective proteins lead to the accumulation of unfolded proteins, a condition referred to as ER stress. ER stress has been reported to induce cellular apoptosis and fibrosis [12,13]. Latest evidence [14–21] has shown that ER stress is involved in the pathogenesis of several cardiovascular diseases such as myocardial ischemia–reperfusion injury, cardiac hypertrophy, diabetic cardiomyopathy, drug induced cardiac injury and cardiac fibrosis. However, the exact role of ER stress in the pathophysiology of infarct-related cardiac rupture or remodeling is unknown.

Therefore, we aimed to investigate the role of ER stress in cardiac rupture and remodeling in the mouse model of MI created by left coronary artery (LCA) permanent ligation with or without 4-phenylbutyric acid (4-PBA), an agent known to attenuate ER stress [22]. Our findings demonstrate that ER stress promotes MI-induced cardiac apoptosis and fibrosis, and that attenuation of ER stress by 4-PBA lessens cardiac rupture and remodeling associated with cardiac apoptosis and fibrosis.

2. Materials and methods

All procedures were performed in accordance with our institutional guidelines for animal research that conforms to the *Guide for the Care and Use of Laboratory Animals* (NIH Publication No. 85-23, revised 1996). The dose/concentration of 4-phenylbutyric acid (4-PBA, Sigma–Aldrich, St. Louis, MO) was determined according to the previous reports [23–

25]. The mice after MI were intraperitoneally injected with 4-PBA every day for 4 weeks at a dose of 20 mg/kg/day (dissolved in 0.9% NaCl).

2.1. Animal models of MI

C57BL/6 male mice (aged 8–12 wks, weighing 20–25 g) were used to generate MI by the permanent ligation of the left coronary artery (LCA) as described elsewhere [5]. The mice were anesthetized with a mixture of xylazine (5 mg/kg, injected i.p.) and ketamine (100 mg/kg, injected i.p.), and the adequacy of anesthesia was monitored from the disappearance of pedal withdrawal reflex. The operated mice that survived for 12 h were randomized to either 4-PBA or 0.9% NaCl administration. Sham-operated mice were also treated with either 4-PBA or 0.9% NaCl.

2.2. Echocardiographic imaging

Transthoracic echocardiographic imaging was performed and the data were analyzed in a blinded manner using a Vevo-770 ultrasonic system (VisualSonics, Toronto, ON, Canada) equipped with a high-resolution transducer centered at 30 MHz and vendor-specific analytic software. The mice in the study were sedated with isoflurane (induction at 3% and maintenance at 0.5–2% in O_2) and placed on a warmed (37 °C) platform. Body temperature, ECG and respiration were monitored. The continuous delivery of isoflurane was titrated to maintain heart rate over 450 bpm. The hearts were scanned using the B-mode, M-mode or Doppler mode imaging at the levels of papillary muscle and mitral valve for cardiac function analysis. Endocardial borders were traced by long-axis and short-axis B mode imaging. From two-dimensionally targeted M-mode tracings, both left ventricular end-diastolic (LVEDd) and end-systolic diameter (LVESd) were measured. Cardiac contractile function was assessed by LV fractional shortening (LVFS%), which was calculated as follows: LVFS $(\%) = (LVEDd - LVESd)/ LVEDd \times 100$. Using Doppler mode imaging, the blood flow velocity through the mitral valve was measured (E and A waves). Cardiac diastolic function was assessed by E/A ratio.

2.3. Autopsy and histology

Autopsy was performed on study animals found dead within the first week of MI, and on surviving animals sacrificed at the indicated time points or after echocardiographic imaging at the end of 4 weeks. The presence of a large amount of blood clot around the heart and in the chest cavity as well as a perforation of the infarcted ventricular wall indicated as the rupture-related death.

After the mice were sacrificed, the hearts were removed from different groups, fixed in 4% paraformaldehyde, embedded in paraffin, and 4 μm sections were prepared for Masson staining to measure the extent of collagen deposition and fibrosis.

2.4. Cell culture

The neonatal Sprague Dawley rats at 1–3 days after birth were anesthetized by 2% isoflurane inhalation. Isolation and culture of ventricular cardiomyocytes and fibroblasts were performed as described elsewhere [26]. Subsequently, both cardiomyocytes and fibroblasts were incubated at 37 °C in either normoxic (5% CO_2 and 20% O_2) or hypoxic

condition (5% CO_2, 3% O_2 and 100% N_2) with or without 4-PBA (0.5 mM) for cell viability assay, mitochondrial membrane potential (Ψm) assay, migration assay for 48, 24 and 72 h respectively. After the exposure to hypoxia, we determined the protein expressions by Western blotting as described below.

2.5. Cell viability assay

4-[3-(4-Idophenyl)-2-(4-nitrophenyl)-2H-5-tetrazolio]-1,3-benzene disulfonate (WST-1) assay for cell viability was used as described elsewhere [27]. Both cultured cardiomyocytes (1×10^5 cells per well) and fibroblasts (1×10^4 cells per well) were placed into 96-well plates with 200 μL of complete culture medium and exposed to either normoxia or hypoxia with or without 4-PBA for 48 h to test the cell viability.

2.6. Mitochondrial membrane potential (Ψm) assay

The mitochondrial membrane potential (Ψm) in the cardiomyocytes was examined by JC-1 staining. JC-1 is a lipophilic, cationic dye that exhibits a fluorescence emission shift upon aggregation from 530 (green monomer) to 590 nm (red "J-aggregates"). In healthy cells with high mitochondrial Ψm, JC-1 enters the mitochondrial matrix in a potential-dependent manner and forms aggregates.

Briefly, the cardiomyocytes (1×10^4) were seeded into confocal glass wells and cultured for 24 h in normoxic or hypoxic condition with or without 4-PBA, then staining was performed using 2.5 μg/ ml JC-1 at 37 °C for 15 min. After staining, the cells were rinsed 3× with phosphate buffered saline (PBS). The dye equilibration was allowed for 10 min at room temperature prior to imaging. The images were observed under Nikon Eclipse Ti-E inverted microscope with a Plan Fluor 10× objective. The samples were illuminated with Nikon C-HGFIE Intensilight (Precentered Fiber Illuminator) and the fluorescence was recorded using Nikon DS-Qi1Mc digital camera. Stained, polarized mitochondria were detected with fluorescence settings for Cy3 (excitation/emission = 50/570 nm, EV = 50 ms). Loss of mitochondrial integrity was detected with the settings for FITC (excitation/emission = 485/535 nm, EV = 500 ms). The images were analyzed using Image J software (NIH) by assessing the red/green fluorescence ratio from the individual image.

2.7. Migration assay

The migration of cardiac fibroblasts was determined using trans-well chambers (24 well trans-well plates inserted with polycarbonate filters, 8-μm pore size, Corning) according to the manufacturer's instruction. The fibroblasts were trypsinized, counted, and loaded equally (1×10^4 cells per well) into the upper chamber of the trans-well plates to incubate for 12 h. When the cells were attached, the upper and lower media was replaced with fresh DMEM alone or with 4-PBA under the normoxic or hypoxic condition. After 72 h incubation, non-migrated cells remained on the upper surface of the membrane were removed with a cotton swab and migrated cells on underside of the membrane were stained with 0.1% crystal violet. The number of migrated cells on each membrane was counted in 5 random fields at 20× magnification under a light microscope.

2.8. Western blot analysis

The proteins were prepared from the whole heart homogenates, primary cultured cardiomyocytes and fibroblasts per published protocols [28]. The immunoblotting was performed using the following primary antibodies: anti-GRP 78 (sc-376768, Santa Cruz), anti-CHOP (#2895, Cell signaling technology), anti-Bax (#2772, Cell Signaling Technology), anti-caspase 3 (#9665, Cell Signaling Technology), anti-TGFβ1 (#3711, Cell Signaling Technology), anti-Smad 2/3 (sc-133098, Santa Cruz) and anti-β-actin (sc-47778, Santa Cruz). Quantification of the images was performed using Image J software (NIH).

2.9. Statistical analysis

All data were expressed as mean ± standard error of the mean (SEM), and $P < 0.05$ were considered as statistically significant. Statistical differences were evaluated by one-way analysis of variance followed by the Bonferroni's multiple comparison exact probability test. The overall survival of the MI mice was evaluated using Kaplan–Meier survival analysis. All analyses were performed using SPSS 13.0 software (SPSS Inc., Chicago, IL).

3. Results

3.1. Cardiac rupture is the major cause of death within the first week of MI

We induced ST-elevation MI by permanent LCA ligation in the mice. Myocardial necrosis after 45 min of occlusion was confirmed by the elevated ST segment on electrocardiogram (ECG) during the surgery as well as detection of the infarcted myocardium (white, nonstained) by triphenyl tetrazolium chloride (TTC) staining (Fig. S1A). Post MI, mice were checked three times a day to ensure that once a dead mouse was found, autopsy was performed immediately to confirm the cause of the death. Our inspection revealed that in post MI day 3–5, cardiac rupture and acute congestive heart failure (CHF) were common. The cardiac rupture was the major cause of death (37.5% rupture rate was observed, see details in Section 3.4). Rupture slits and blood clots around the heart of the mice were observed (Fig. S1B). Consistent with acute CHF, pulmonary and atrial congestion were apparent in dead mice (Fig. S1C).

3.2. Cardiac remodeling is prevalent in the late phase of MI

Negative cardiac remodeling is one of the most common pathophysiological outcomes after survival of MI. We characterized cardiac remodeling in the mice that survived the acute period post MI. Examination of the gross specimen and cross sections of the heart showed left ventricular (LV) chamber enlargement as early as day 1 post MI, while myocardial fibrosis per Masson staining was detected 3 days after MI and worsened through day 28 (Fig. S2A and B). There was a large ventricular aneurysm formed at the end of 28 days, as shown representatively in Fig. S2C. Both LVEDd and LVESd were increased as measured by echocardiography, attesting to chamber enlargement and LVFS impairment (Fig. S2D; Table S1). Meanwhile, the mitral inflow E wave velocity was increased post MI along with the markedly decreased A wave in mice that survived the MI to the end of 28 days (Table S1). E/A ratio therefore significantly increased as a restrictive filling state. These findings demonstrate extensive negative cardiac remodeling that occurs after survival from MI and

includes the left ventricle dilation and deformation as well as impairment of both systolic and diastolic function of the heart.

3.3. ER stress induces cardiac apoptosis and fibrosis in mice in the development of MI

To test whether ER stress is one of the underlying mechanisms involved in the cardiac rupture and remodeling, we investigated the protein expression profile of ER stress markers (GRP 78 and CHOP), pro-apoptotic proteins (Bax and caspase 3) and pro-fibrotic proteins (TGF-β1 and Smad 2/3) in the whole homogenates of the mouse hearts in both early and late phases of MI. The protein level of GRP 78 and CHOP were significantly increased from day 1 of MI and remained elevated for the following 4 weeks (Fig. 1A), indicating that the ER stress response is activated acutely and sustained throughout the 4 weeks post MI. Interestingly, we found different expression modes of pro-apoptotic and pro-fibrotic proteins in this process: The expression of the pro-apoptotic markers, Bax and caspase 3, was acutely increased post MI, peaking at the 3rd day and sharply fell to that similar to sham surgery (Fig. 1B). However, the pro-fibrotic marker, TGFβ1 and Smad 2/3, were mainly expressed in the late phase of MI, with the protein levels continuing to rise at day 28 (Fig. 1C). Therefore, the pro-apoptotic markers we examined were induced during the acute phase of the post-MI period when the majority of myocyte death is to occur due to the infarct-related insult, while the pro-fibrotic marker upregulation correlated with subacute/late phase, during which time negative remodeling of the left ventricle takes place.

We then examined whether the attenuation of ER stress alleviated cardiac apoptosis and/or fibrosis in the early and late phase of MI by studying the effect of ER stress attenuation on the expression levels of these marker proteins differentially expressed in the post-MI time period. We intraperitoneally administrated 4-PBA (20 mg/ kg/d), a commonly used ER stress inhibitor [22], after MI for 3 days and 28 days respectively. Our results showed that 4-PBA decreased the protein level of CHOP, Bax and caspase 3 at 3rd day of MI (Fig. 1D), while at 28th day of MI, it markedly lowered the protein level of CHOP, TGFβ1 and Smad 2/3 (Fig. 1E). Together, these findings suggest that the ER stress responses following MI occur early at the time of cardiac apoptosis and persist during the subacute/ late phase of fibrosis, and that the attenuation of ER stress inhibits expression of molecular markers strongly associated with acute cardiac cell death and late-phase fibrosis.

3.4. 4-PBA prevents cardiac rupture and attenuates cardiac remodeling in MI mice

We further tested whether attenuation of ER stress responses by 4-PBA has impact on the extent of MI and remodeling at the organ level, and ultimately on the survival rate of mice post MI. We found that 4-PBA treatment improved the extent of infarct and cardiac remodeling, as indicated by smaller ventricular aneurysm and less myocardial fibrosis (Fig. 2A). Amelioration of the infarct and remodeling was also associated with increased systolic function, represented by higher fractional shortening of the left ventricle, as well as improvement in diastolic function with normalized E/A ratio (Fig. 2B and Table S2). As shown in Fig. 2C, these positive effects of 4-PBA at the organ level was associated with higher overall survival rate of the mice treated with 4-PBA when compared to the vehicle group (76.2% *vs*. 47.5%, $P = 0.042$). Twenty-one mice were found dead (52.5%) in 40 vehicle-treated mice, among which the mice with cardiac rupture accounted for 37.5%

(15/40) and the mice with signs of acute HF accounted for 15% (6/40). However, there was only 5 dead (22.7%) in the 22 mice receiving 4-PBA after MI, among which those with cardiac rupture accounted for 18.2% (4/22) and acute HF 4.5% (1/22). Using Kaplan–Meier analysis, we found that 4-PBA significantly lowered the incidence of cardiac rupture and HF and increased survival at the end of 28 days. Thus, the attenuation of ER stress via treatment with 4-PBA led to amelioration of cardiac rupture and remodeling, protection from deterioration of left ventricular function and overall better survival in mice post MI.

3.5. 4-PBA protects cultured cardiomyocytes from apoptosis induced by hypoxia

To investigate the cellular mechanisms underlying the protection conferred by 4-PBA, neonatal rat cardiomyocytes were exposed to hypoxia to simulate ischemic injury *in vitro* in the presence or absence of 4-PBA (0.5 mM) and cell viability was tested by a WST1 assay per published protocols [29]. Hypoxia for 48 h reduced the cellular viability with the associated increase in the expression of CHOP, Bax and caspase 3, all of which were attenuated by 4-PBA (Fig. 3A and B). Since the changes of mitochondrial potential is one of the first signs of apoptosis, we determined the mitochondrial depolarization using JC-1 staining in cultured cardiomyocytes exposed to hypoxia (for 24 h to maximize detection of cells in the early phase of apoptosis, rather than the previous 48 h of hypoxia) with or without 4-PBA (Fig. 3C). Hypoxia significantly decreased the mitochondrial red/green fluorescence intensity ratio, indicating altered mitochondrial membrane potential and depolarization. 4-PBA treatment partly recovered the mitochondrial red/green fluorescence intensity ratio, suggesting that it provides protection against mitochondrial depolarization induced by hypoxia.

3.6. 4-PBA inhibits the proliferation and migration of cultured cardiac fibroblasts induced by hypoxia

In order to explore the cellular mechanisms associated with the ameliorated cardiac remodeling provided by 4-PBA, we assessed the proliferation and migration of fibroblasts during hypoxia. The duration of hypoxia was 72 h, which was an optimal length of time for detection of proliferation and migration of fibroblasts under hypoxic stress (*unpublished observation*). The results of the viability assay via WST-1 and Western blots showed that hypoxia in fact increased the proliferation of fibroblasts (in contrast to its effect on cardiomyocytes) and increased the expression of CHOP, TGFβ1 and Smad 2/3, all of which were inhibited by 4-PBA (Fig. 4A and B). Using a well-established trans-well migration system [30], we determined the extent of fibroblast migration under hypoxia. As shown in Figs. 4C, hypoxia increased the migration of fibroblasts, which was attenuated by 4-PBA. These findings indicate that ER stress attenuation by 4-PBA inhibits hypoxia-induced proliferation and migration of cardiac fibroblasts. This suppressive action on the fibroblasts may provide an important mechanism behind the significantly reduced ventricular fibrosis and negative remodeling afforded by 4-PBA.

4. Discussion

The role of ER stress in cardiovascular diseases has been reported for decades but never therapeutically targeted in myocardial infarction. In this study using a murine MI model, we

provide strong physiological and cellular data demonstrating that attenuation of ER stress prevents infarct-induced cardiac rupture and remodeling by modulating both cardiac apoptosis and fibrosis.

After MI or hypoxia, the ER stress responses occur in cardiac cells as the results of reduced oxygen supply, reduced calcium levels, insufficient concentrations of molecular chaperones, altered protein glycosylation machinery, altered redox status and so on within the ER lumen. It then leads to the initiation of the unfolded protein response (UPR), an adaptive mechanism that promotes organelle recovery [31]. However, if ER stress is prolonged or uncontrolled, cell death, rather than recovery, can ensue by CHOP-induced apoptosis [32].

Cardiac rupture and negative remodeling following MI worsen morbidity and mortality due to cardiomyocyte necrosis, apoptosis and myocardial fibrosis [33,34]. It has been purported that ER stress may play a crucial role in the pathogenesis of these detrimental sequelae, with the GRP78-PERK-CHOP cross-talk at its center [35–37]. Our results demonstrated that (1) ER stress responses, indicated by GRP78 and CHOP expression, in the ischemic heart were acutely increased in the early phase of MI and persisted through the following four weeks, (2) the attenuation of ER stress by 4-PBA decreased the expression of proteins involved not only in the ER stress response (CHOP), but in apoptosis (Bax and caspase 3) and fibrosis (TGFβ1 and Smad 2/3), and (3) these molecular changes after treatment with 4-PBA were associated with better left ventricular function, less negative remodeling and better survival of the animals, indicating that ER stress plays a central role in cardiac cell death and fibrosis in the development of acute and chronic sequelae post MI. Our cultured cell model of hypoxia-simulated ischemia also supports the protective effects of 4-PBA on cardiomyocyte survival, closely linked with the mitochondrial membrane integrity. We also demonstrate the suppressive effect of 4-PBA on fibroblast migration and viability, which may account for, in part, the reduction seen in the negative remodeling and fibrosis of the heart with the treatment with 4-PBA.

Uncontrolled ER stress responses are also associated with the activated inflammasome in chronic inflammatory diseases [38]. And it is known that suppression of inflammatory cytokines is one of the mechanisms associated with beneficial effects of 4-PBA [39]. However, the detailed connection between ER stress and inflammation in the development of adverse sequelae post MI remains largely unexplored and still need to investigate in the future study. Aside from its effect on the myocardial cells, it is possible that the protective effects of 4-PBA may in part derive from improved vascular endothelial function related to ER stress inhibition in reducing the MI-induced cardiac rupture and post-infarct remodeling [40]. We hope to differentiate and elucidate further these possible mechanisms in the future.

4-PBA has been approved by US Food and Drug Administration (FDA) for clinical use as an ammonia scavenger in children with urea cycle disorders [41]. It is a low-molecular-weight fatty acid and a non-toxic pharmacological compound found to have chaperone-like activity [42], and its effectiveness was also shown to be associated with inhibition of histone deacetylase (HDAC) [43,44]. 4-PBA was used as an anti-cancer drug in patients with advanced solid tumors because of its role in the epigenetic regulation of protein translation by HDAC inhibition [45]. In fact, inhibition of HDAC has been shown to promote

Author Manuscript

Author Manuscript

Author Manuscript

Author Manuscript

myocardial repair and protect against the cardiac remodeling after MI [46]. The inhibition of HDAC by high dosage of 4-PBA (400 mg/kg/d) has also been shown to protect against adriamycin-induced cardiac injury in mice [20]. However, its effect on HDAC inhibition is dose-dependent, and the use of the lower dose (20 mg/kg/d) of 4-PBA in this study allowed us to examine its action on ER stress in the context of MI, with little effects on HDAC inhibition (*unpublished observation*).

In conclusion, our results demonstrate a sustained ER stress response associated with cardiac apoptosis and fibrosis post infarction, and show for the first time that attenuation of ER stress using 4-PBA is an effective agent to limit the extent of MI and prevent infarct-induced cardiac rupture and remodeling to preserve cardiac function and overall survival.

Supplementary Material

Refer to Web version on PubMed Central for supplementary material.

Acknowledgments

References

1. Gao XM, White DA, Dart AM, Du XJ. Post-infarct cardiac rupture: recent insights on pathogenesis and therapeutic interventions. Pharmacol Ther. 2012; 134:156–179. [PubMed: 22260952]

2. Becker RC, Gore JM, Lambrew C, Weaver WD, Rubison RM, French WJ, Tiefenbrunn AJ, Bowlby LJ, Rogers WJ. A composite view of cardiac rupture in the United States National Registry of Myocardial Infarction. J Am Coll Cardiol. 1996; 27:1321–1326. [PubMed: 8626938]

3. Lopez-Sendon J, Gonzalez A, Lopez de Sa E, Coma-Canella I, Roldan I, Dominguez F, Maqueda I, Martin Jadraque L. Diagnosis of subacute ventricular wall rupture after acute myocardial infarction: sensitivity and specificity of clinical, hemodynamic and echocardiographic criteria. J Am Coll Cardiol. 1992; 19:1145–1153. [PubMed: 1564213]

4. Lal H, Zhou J, Ahmad F, Zaka R, Vagnozzi RJ, Decaul M, Woodgett J, Gao E, Force T. Glycogen synthase kinase-3alpha limits ischemic injury, cardiac rupture post-myocardial infarction remodeling and death. Circulation. 2012; 125:65–75. [PubMed: 22086876]

5. Gao XM, Xu Q, Kiriazis H, Dart AM, Du XJ. Mouse model of post-infarct ventricular rupture: time course, strain- and gender-dependency, tensile strength and histopathology. Cardiovasc Res. 2005; 65:469–477. [PubMed: 15639486]

6. Braunwald E. Heart failure. JACC Heart Fail. 2013; 1:1–20. [PubMed: 24621794]

7. Jugdutt BI. Ischemia/infarction. Heart Fail Clin. 2012; 8:43–51. [PubMed: 22108726]

8. Griffiths HR, Dias IH, Willetts RS, Devitt A. Redox regulation of protein damage in plasma. Redox Biol. 2014; 2:430–435. [PubMed: 24624332]

9. Malhotra JD, Kaufman RJ. Endoplasmic reticulum stress and oxidative stress: a vicious cycle or a double-edged sword? Antioxid Redox Signal. 2007; 9:2277–2293. [PubMed: 17979528]

10. Groenendyk J, Agellon LB, Michalak M. Coping with endoplasmic reticulum stress in the cardiovascular system. Annu Rev Physiol. 2013; 75:49–67. [PubMed: 23020580]

11. Paschen W. Role of calcium in neuronal cell injury: which subcellular compartment is involved? Brain Res Bull. 2000; 53:409–413. [PubMed: 11136996]

12. Schroder M, Kaufman RJ. The mammalian unfolded protein response. Annu Rev Biochem. 2005; 74:739–789. [PubMed: 15952902]

13. Minamino T, Komuro I, Kitakaze M. Endoplasmic reticulum stress as a therapeutic target in cardiovascular disease. Circ Res. 2010; 107:1071–1082. [PubMed: 21030724]

14. Tao J, Zhu W, Li Y, Xin P, Li J, Liu M, Li J, Redington AN, Wei M. Apelin-13 protects the heart against ischemia–reperfusion injury through inhibition of ER-dependent apoptotic pathways in a time-dependent fashion. Am J Physiol Heart Circ Physiol. 2011; 301:H1471–H1486. [PubMed: 21803944]

15. Chen YH, Wu XD, Yao ST, Sun S, Liu XH. Calcineurin is involved in cardioprotection induced by ischemic postconditioning through attenuating endoplasmic reticulum stress. Chin Med J (Engl). 2011; 124:3334–3340. [PubMed: 22088531]

16. Park CS, Cha H, Kwon EJ, Sreenivasaiah PK, Kim do H. The chemical chaperone 4-phenylbutyric acid attenuates pressure-overload cardiac hypertrophy by alleviating endoplasmic reticulum stress. Biochem Biophys Res Commun. 2012; 421:578–584. [PubMed: 22525677]

17. Ji Y, Zhao Z, Cai T, Yang P, Cheng M. Liraglutide alleviates diabetic cardiomyopathy by blocking CHOP-triggered apoptosis via the inhibition of the IRE-alpha pathway. Mol Med Rep. 2014; 9:1254–1258. [PubMed: 24535553]

18. Liu ZW, Zhu HT, Chen KL, Dong X, Wei J, Qiu C, Xue JH. Protein kinase RNA-like endoplasmic reticulum kinase (PERK) signaling pathway plays a major role in reactive oxygen species (ROS)-mediated endoplasmic reticulum stress-induced apoptosis in diabetic cardiomyopathy. Cardiovasc Diabetol. 2013; 12:158. [PubMed: 24180212]

19. Shi FH, Cheng YS, Dai DZ, Peng HJ, Cong XD, Dai Y. Depressed calcium-handling proteins due to endoplasmic reticulum stress and apoptosis in the diabetic heart are attenuated by argirein. Naunyn Schmiedebergs Arch Pharmacol. 2013; 386:521–531. [PubMed: 23525487]

20. Daosukho C, Chen Y, Noel T, Sompol P, Nithipongvanitch R, Velez JM, Oberley TD, St Clair DK. Phenylbutyrate, a histone deacetylase inhibitor, protects against adriamycin-induced cardiac injury. Free Radic Biol Med. 2007; 42:1818–1825. [PubMed: 17512461]

21. Ayala P, Montenegro J, Vivar R, Letelier A, Urroz PA, Copaja M, Pivet D, Humeres C, Troncoso R, Vicencio JM, Lavandero S, Lavandero G. Attenuation of endoplasmic reticulum stress using the chemical chaperone 4-phenylbutyric acid prevents cardiac fibrosis induced by isoproterenol. Exp Mol Pathol. 2012; 92:97–104. [PubMed: 22101259]

22. Basseri S, Lhotak S, Sharma AM, Austin RC. The chemical chaperone 4-phenylbutyrate inhibits adipogenesis by modulating the unfolded protein response. J Lipid Res. 2009; 50:2486–2501. [PubMed: 19461119]

23. Qi W, Mu J, Luo ZF, Zeng W, Guo YH, Pang Q, Ye ZL, Liu L, Yang FH, Feng B. Attenuation of diabetic nephropathy in diabetes rats induced by streptozotocin by regulating the endoplasmic reticulum stress inflammatory response. Metabolism. 2011; 60:594–603. [PubMed: 20817186]

24. Srinivasan K, Sharma SS. Sodium phenylbutyrate ameliorates focal cerebral ischemic/reperfusion injury associated with comorbid type 2 diabetes by reducing endoplasmic reticulum stress and DNA fragmentation. Behav Brain Res. 2011; 225:110–116. [PubMed: 21767572]

25. Wang JQ, Chen X, Zhang C, Tao L, Zhang ZH, Liu XQ, Xu YB, Wang H, Li J, Xu DX. Phenylbutyric acid protects against carbon tetrachloride-induced hepatic fibrogenesis in mice. Toxicol Appl Pharmacol. 2013; 266:307–316. [PubMed: 23174480]

26. Xuan W, Liao Y, Chen B, Huang Q, Xu D, Liu Y, Bin J, Kitakaze M. Detrimental effect of fractalkine on myocardial ischaemia and heart failure. Cardiovasc Res. 2011; 92:385–393. [PubMed: 21840883]

27. Vietti G, Ibouraadaten S, Palmai-Pallag M, Yakoub Y, Bailly C, Fenoglio I, Marbaix E, Lison D, van den Brule S. Towards predicting the lung fibrogenic activity of nanomaterials: experimental validation of an in vitro fibroblast proliferation assay. Part Fibre Toxicol. 2013; 10:52. [PubMed: 24112397]

28. Matsubara H, Kanasaki M, Murasawa S, Tsukaguchi Y, Nio Y, Inada M. Differential gene expression and regulation of angiotensin II receptor subtypes in rat cardiac fibroblasts and cardiomyocytes in culture. J Clin Invest. 1994; 93:1592–1601. [PubMed: 8163661]

29. Kacimi R, Long CS, Karliner JS. Chronic hypoxia modulates the interleukin-1beta-stimulated inducible nitric oxide synthase pathway in cardiac myocytes. Circulation. 1997; 96:1937–1943. [PubMed: 9323084]

30. Justus CR, Leffler N, Ruiz-Echevarria M, Yang LV. In vitro cell migration and invasion assays. J Vis Exp. 2014; 1:88.

31. Doroudgar S, Glembotski CC. New concepts of endoplasmic reticulum in the heart: programmed to conserve. J Mol Cell Cardiol. 2013; 55:85–91. [PubMed: 23085588]

32. Liu D, Zhang M, Yin H. Signaling pathways involved in endoplasmic reticulum stress-induced neuronal apoptosis. Int J Neurosci. 2013; 123:155–162. [PubMed: 23134425]

33. Foster CR, Daniel LL, Daniels CR, Dalal S, Singh M, Singh K. Deficiency of ataxia telangiectasia mutated kinase modulates cardiac remodeling following myocardial infarction: involvement in fibrosis and apoptosis. PLoS One. 2013; 8:e83513. [PubMed: 24358288]

34. Unsold B, Kaul A, Sbroggio M, Schubert C, Regitz-Zagrosek V, Brancaccio M, Damilano F, Hirsch E, Van Bilsen M, Munts C, Sipido K, Bito V, Detre E, Wagner NM, Schafer K, Seidler T, Vogt J, Neef S, Bleckmann A, Maier LS, Balligand JL, Bouzin C, Ventura-Clapier R, Garnier A, Eschenhagen T, El-Armouche, Knoll R, Tarone G, Hasenfuss G. Melusin protects from cardiac rupture and improves functional remodelling after myocardial infarction. Cardiovasc Res. 2014; 101:97–107. [PubMed: 24130190]

35. Chen YJ, Su JH, Tsao CY, Hung CT, Chao HH, Lin JJ, Liao MH, Yang ZY, Huang HH, Tsai FJ, Weng SH, Wu YJ. Sinulariolide induced hepatocellular carcinoma apoptosis through activation of mitochondrial-related apoptotic and PERK/eIF2alpha/ATF4/CHOP pathway. Molecules. 2013; 18:10146–10161. [PubMed: 23973991]

36. Chiang CK, Hsu SP, Wu CT, Huang JW, Cheng HT, Chang YW, Hung KY, Wu KD, Liu SH. Endoplasmic reticulum stress implicated in the development of renal fibrosis. Mol Med. 2011; 17:1295–1305. [PubMed: 21863214]

37. Tan TC, Crawford DH, Jaskowski LA, Subramaniam VN, Clouston AD, Crane DI, Bridle KR, Anderson GJ, Fletcher LM. Excess iron modulates endoplasmic reticulum stress-associated pathways in a mouse model of alcohol and high-fat diet-induced liver injury. Lab Invest. 2013; 93:1295–1312. [PubMed: 24126888]

38. Menu P, Mayor A, Zhou R, Tardivel A, Ichijo H, Mori K, Tschopp J. ER stress activates the NLRP3 inflammasome via an UPR-independent pathway. Cell Death Dis. 2012; 3:e261. [PubMed: 22278288]

39. Zeng W, Guo YH, Qi W, Chen JG, Yang LL, Luo ZF, Mu J, Feng B. 4-Phenylbutyric acid suppresses inflammation through regulation of endoplasmic reticulum stress of endothelial cells stimulated by uremic serum. Life Sci. 2014; 103:15–24. [PubMed: 24650493]

40. Galán M, Kassan M, Kadowitz PJ, Trebak M, Belmadani S, Matrougui K. Mechanism of endoplasmic reticulum stress-induced vascular endothelial dysfunction. Biochim Biophys Acta. 2014; 1843:1063–1075. [PubMed: 24576409]

41. Maestri NE, Brusilow SW, Clissold DB, Bassett SS. Long-term treatment of girls with ornithine transcarbamylase deficiency. N Engl J Med. 1996; 335:855–859. [PubMed: 8778603]

42. Ricobaraza A, Cuadrado-Tejedor M, Marco S, Perez-Otano I, Garcia-Osta A. Phenylbutyrate rescues dendritic spine loss associated with memory deficits in a mouse model of Alzheimer disease. Hippocampus. 2012; 22:1040–1050. [PubMed: 21069780]

43. Kim SW, Hooker JM, Otto N, Win K, Muench L, Shea C, Carter P, King P, Reid AE, Volkow ND, Fowler JS. Whole-body pharmacokinetics of HDAC inhibitor drugs, butyric acid, valproic acid and 4-phenylbutyric acid measured with carbon-11 labeled analogs by PET. Nucl Med Biol. 2013; 40:912–918. [PubMed: 23906667]

44. Camacho LH, Olson J, Tong WP, Young CW, Spriggs DR, Malkin MG. Phase I dose escalation clinical trial of phenylbutyrate sodium administered twice daily to patients with advanced solid tumors. Invest New Drugs. 2007; 25:131–138. [PubMed: 17053987]

45. Camacho LH, Olson J, Tong WP, Young CW, Spriggs DR, Malkin MG. Phase I dose escalation clinical trial of phenylbutyrate sodium administered twice daily to patients with advanced solid tumors. Invest New Drugs. 2006; 25:131–138. [PubMed: 17053987]

46. Zhang L, Chen B, Zhao Y, Dubielecka PM, Wei L, Qin GJ, Chin YE, Wang Y, Zhao TC. Inhibition of histone deacetylase-induced myocardial repair is mediated by c-kit in infarcted hearts. J Biol Chem. 2012; 287:39338–39348. [PubMed: 23024362]

Appendix A. Supplementary data

Supplementary data associated with this article can be found, in the online version, at http://dx.doi.org/10.1016/j.cbi.2014.10.032.

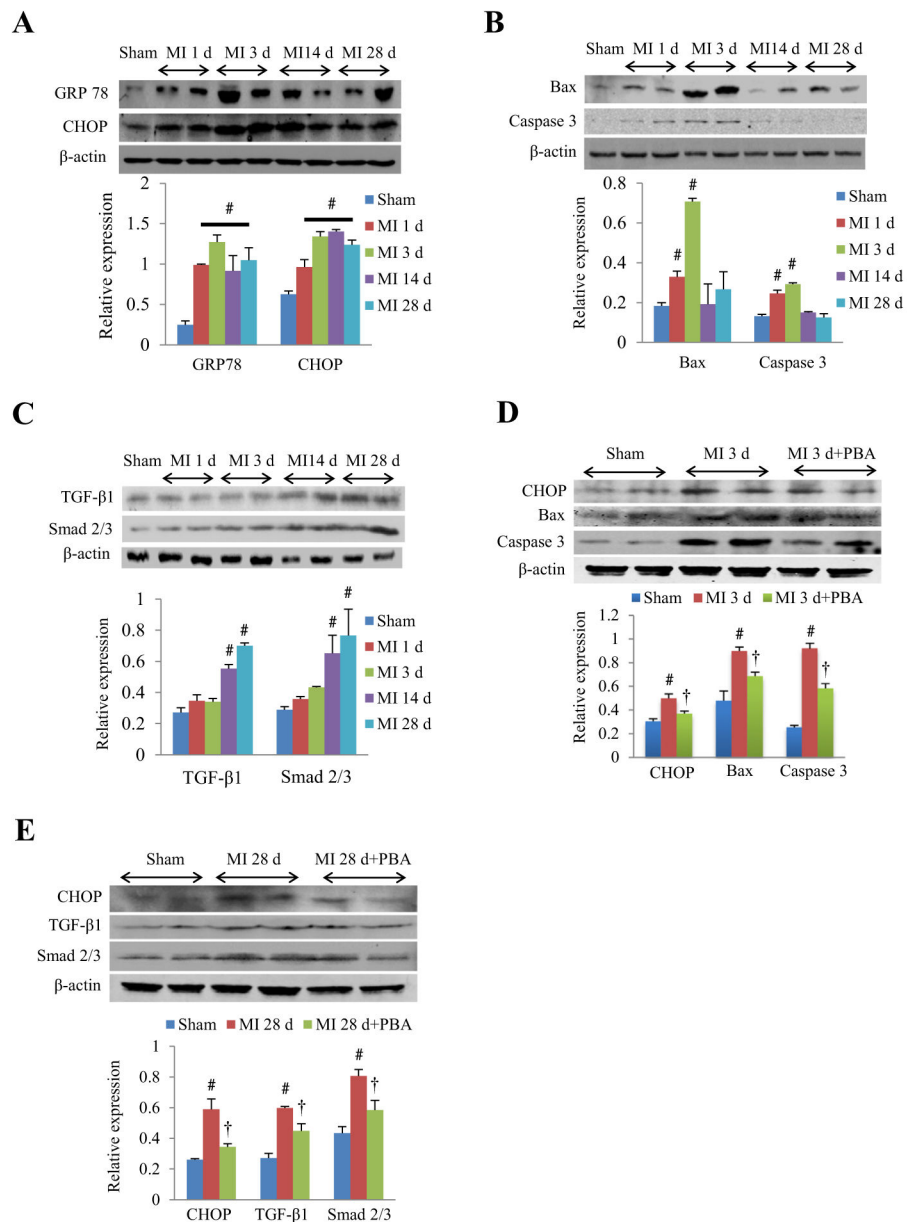Author Manuscript Author Manuscript Author Manuscript Author Manuscript

Fig. 1.
ER stress response in cardiac apoptosis and fibrosis after MI. (A) Western blots and quantitative analysis of ER stress response markers (GRP 78 and CHOP) in the whole heart homogenates of mice in the early and late phase of MI. (B) Western blots and quantitative analysis of pro-apoptotic proteins (Bax and caspase 3) in the whole heart homogenates of mice in the early and late phase of MI. (C) Western blots and quantitative analysis of pro-fibrotic proteins (TGF-β1 and Smad 2/3) in the whole heart homogenates of mice in the early and late phase of MI. (D) Representative Western blots and quantitative analysis of CHOP, Bax and caspase 3 from whole heart homogenates at 3rd day of MI with or without 4-PBA (20 mg/kg/d). (E) Representative Western blots and quantitative analysis of CHOP,

TGF-β1 and Smad 2/3 from whole heart homogenates at 28th day of MI with or without 4-PBA (20 mg/kg/d). $^{\#}P < 0.05$ vs. sham; $^{\dagger}P < 0.05$ vs. MI; $n = 4$–6 in each group.
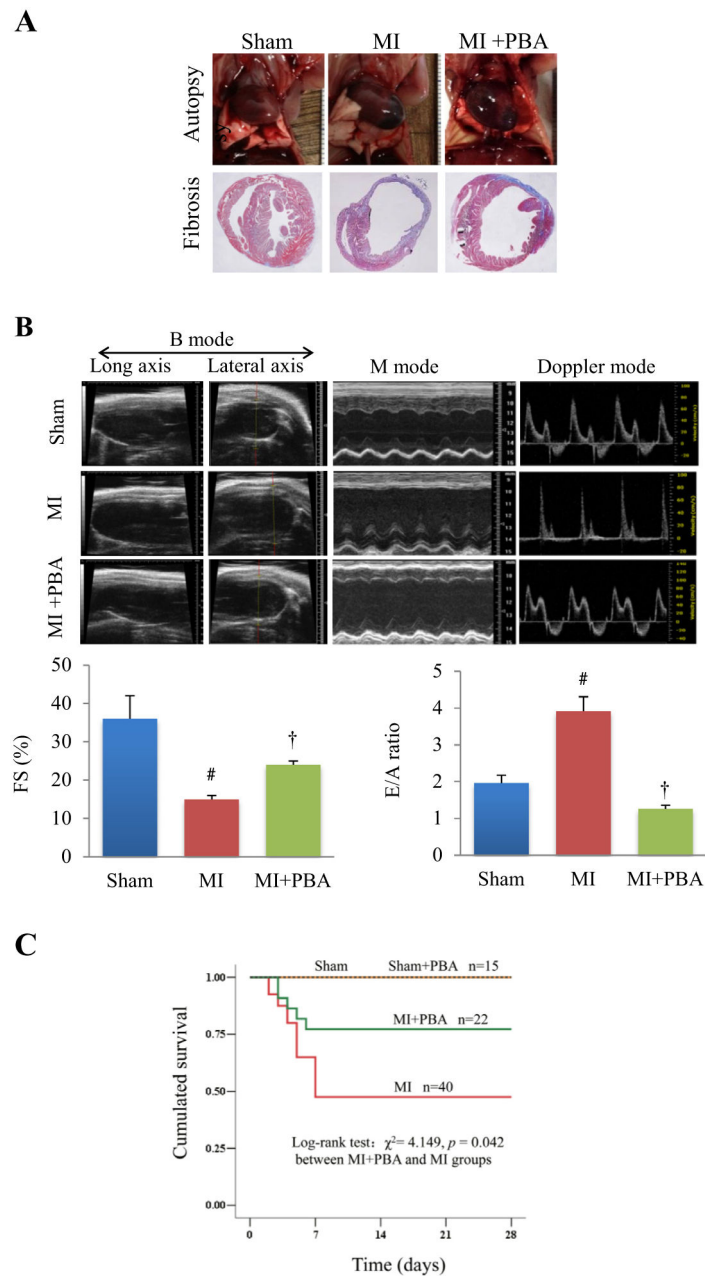
Fig. 2.
Effects of 4-PBA treatment on the cardiac remodeling, cardiac function, and survival rate in MI mice. (A) Representative autopsy pictures of ventricular aneurysm and Masson staining of myocardial fibrosis from the hearts of mice with or without 4-PBA administration at the end of 4 weeks post MI. (B) Representative echocardiographic imaging of mice after sham surgery, MI and 4-PBA + MI is presented, with quantitative analysis of fractional shortening (FS%) and E/A ratio (top, lower left, lower right, respectively). #$P < 0.01$ vs. sham; †$P < 0.01$ vs. MI. (C) Four-week survival rate of the mice with or without 4-PBA treatment following MI. $n = 15$ each in Sham and Sham + PBA group, $n = 40$ in MI group and $n = 22$ in MI + PBA group.
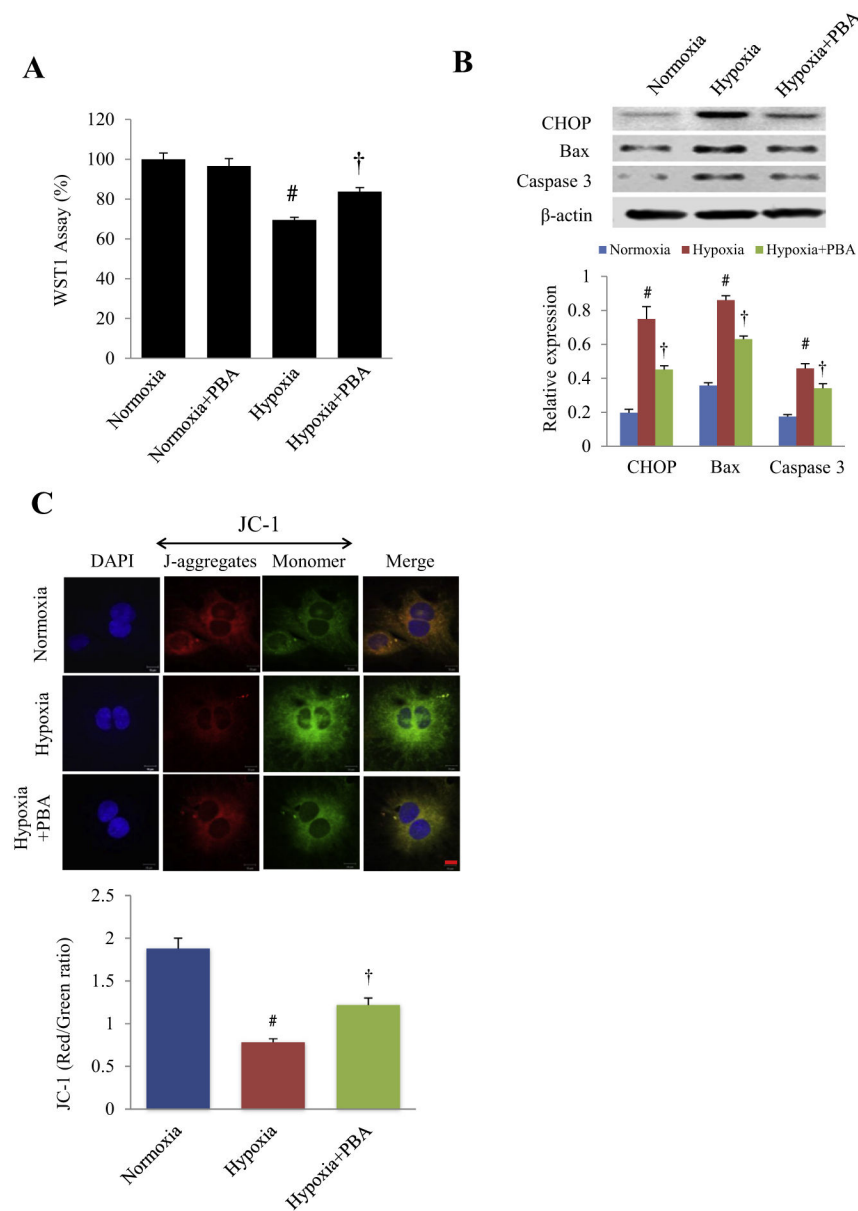
Fig. 3.

Effects of 4-PBA treatment on cell viability in cultured neonatal rat cardiomyocytes under hypoxia. (A) After 48 h of hypoxia, the viability of cardiomyocytes was measured by the WST1 assay. $^{\#}P < 0.01$ vs. Normoxia; $^{\dagger}P < 0.01$ vs. Hypoxia; $n = 15$ (plate holes) in each group. (B) Representative Western blots and quantitative analysis of CHOP, Bax and caspase 3 protein expression in cultured cardiomyocytes after hypoxia for 48 h. $^{\#}P < 0.05$ vs. normoxia; $^{\dagger}P < 0.05$ vs. hypoxia; $n = 5$ independent experiments. (C) After 24 h of hypoxia, mitochondrial membrane potential was analyzed by JC-1 staining (top) and assessing the ratio of the fluorescence intensity between the red J-aggregate and green monomer fluorescence, with quantitative analysis of the ratio (bottom). Scale bar, 10 μm. $^{\#}P < 0.05$ vs. normoxia; $^{\dagger}P < 0.05$ vs. hypoxia; $n = 3$ independent experiments. (For

interpretation of the references to color in this figure legend, the reader is referred to the web version of this article.)
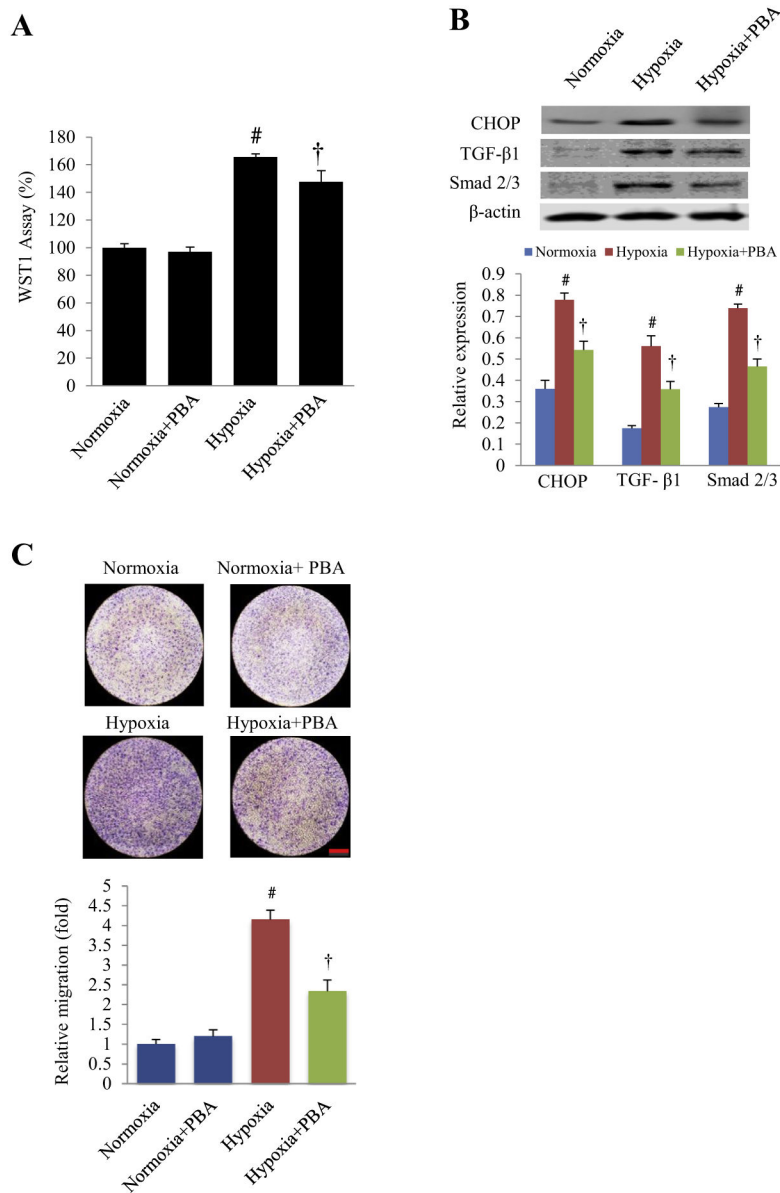
Fig. 4.
Effects of 4-PBA treatment on proliferation and migration of cultured neonatal rat cardiac fibroblast under hypoxia. (A) After 72 h of hypoxia (3% oxygen), the viability of neonatal rat cardiac fibroblasts was measured by the WST1 assay with or without 4-PBA treatment. [#]$P < 0.01$ vs. normoxia; [†]$P < 0.01$ vs. hypoxia; $n = 15$ (plate holes). (B) Representative Western blots and quantitative analysis of CHOP, TGF-β1 and Smad 2/3 in the cultured cardiac fibroblasts under hypoxia for 72 h. [#]$P < 0.05$ vs. normoxia; [†]$P < 0.05$ vs. hypoxia; $n = 5$. (C) Cell migration was detected by transwell migration assay. After 72 h of hypoxia with or without 4-PBA, fibroblasts in the inner membrane of transwell chamber were wiped away. After the transwell membranes were dry, the opposite side of the membrane was stained by crystal violet to detect the migrated cells (top) with quantitative

analysis of fibroblast migration (bottom). [#]$P < 0.05$ vs. normoxia; [†]$P < 0.05$ vs. hypoxia; $n = 3$ in each group. Scale bar, 1 mm.